Cerebral Cortex October 2006;16:1418-1430
doi:10.1093/cercor/bhj079
Advance Access publication November 23, 2005

Connection Patterns Distinguish 3 Regions of Human Parietal Cortex

M. F. S. Rushworth[1,2], T. E. J. Behrens[2] and H. Johansen-Berg[2]

[1]Department of Experimental Psychology, University of Oxford, South Parks Road, Oxford OX1 3UD, UK and [2]Centre for Functional Magnetic Resonance Imaging of the Brain, Department of Clinical Neurology, University of Oxford, John Radcliffe Hospital, Headley Way, Oxford OX3 9DU, UK

Three regions of the macaque inferior parietal lobule and adjacent lateral intraparietal sulcus (IPS) are distinguished by the relative strengths of their connections with the superior colliculus, parahippocampal gyrus, and ventral premotor cortex. It was hypothesized that connectivity information could therefore be used to identify similar areas in the human parietal cortex using diffusion-weighted imaging and probabilistic tractography. Unusually, the subcortical routes of the 3 projections have been reported in the macaque, so it was possible to compare not only the terminations of connections but also their course. The medial IPS had the highest probability of connection with the superior colliculus. The projection pathway resembled that connecting parietal cortex and superior colliculus in the macaque. The posterior angular gyrus and the adjacent superior occipital gyrus had a high probability of connection with the parahippocampal gyrus. The projection pathway resembled the macaque inferior longitudinal fascicle, which connects these areas. The ventral premotor cortex had a high probability of connection with the supramarginal gyrus and anterior IPS. The connection was mediated by the third branch of the superior longitudinal fascicle, which interconnects similar regions in the macaque. Human parietal areas have anatomical connections resembling those of functionally related macaque parietal areas.

Keywords: anatomical projections, attention, macaque, parahippocampal gyrus, parietal cortex, premotor cortex, superior colliculus

Introduction

The inferior parietal lobule (IPL) and the adjacent lateral bank of the intraparietal sulcus (IPS) of the macaque brain are partitioned into distinct functional areas (Geyer and others 2000). Neuroimaging techniques such as functional magnetic resonance imaging (fMRI) have been employed in attempts to identify human parietal regions with similar functional characteristics, but aspects of comparative anatomical organization remain unclear (Corbetta and Shulman 2002; Fink and Grefkes 2005). In the present investigation, we took the distinct approach of attempting to identify in the human brain anatomical connection patterns that are associated with 3 regions of the macaque IPL and the adjacent lateral IPS.

In the macaque, the IPS is the major anatomical structure in the region, and the naming of many parietal areas refers to their position with respect to the IPS. The lateral intraparietal area (LIP) and the anterior intraparietal area (AIP) occupy the posterior and anterior parts of the lateral bank of the IPS, respectively (Fig. 1). Two principle regions 7a or PG and 7b or PF occupy much of the posterior and anterior parts of IPL, respectively (Brodmann 1909; Von Bonin and Bailey 1947; Pandya and Seltzer 1982; Geyer and others 2000). A transitional region between the two main divisions, PFG, a very posterior area Opt, and some transitional opercular regions in the most ventral part of the IPL are also recognized. Distinct functional and anatomical regions, MIP and PE, occupy the medial bank of the IPS and the superior parietal lobule (SPL).

The functional specializations of these regions have been investigated with electrophysiology in macaque and imaging and lesions studies in the human brain. AIP neurons are active when monkeys move the hand or see graspable objects (Sakata and others 1997), and on the basis of lesion and neuroimaging data, it has been argued that a similar functional region can be identified in the anterior lateral bank of the human IPS (Binkofski and others 1998; Binkofski, Buccino, Posse, and others 1999; Grefkes and others 2002; Shikata and others 2003). LIP neurons are active during eye movements or covert shifts of attention (Colby and Duhamel 1991; Andersen and Buneo 2002). A region with similar functional characteristics can be identified in the human brain (Nobre and others 1997; Grosbras and others 2005), but it has puzzling characteristics and its location may indicate differences between parietal organization in the human and macaque. On the one hand, as in the monkey, the human region concerned with visuospatial attention and eye movements lies lateral and ventral to a medial and superior region concerned with arm movements and motor intentions (Rushworth, Paus, and Sipila 2001; Astafiev and others 2003). On the other hand, high–spatial resolution studies in individual subjects suggest that the region is located in the medial rather than the lateral bank of the IPS (Sereno and others 2001; Astafiev and others 2003; Koyama and others 2004). Attentional modulation is also seen in more posterior and ventral medial IPS close to the transverse occipital sulcus (Corbetta and others 2000; Rushworth, Paus, and Sipila 2001; Grosbras and others 2005; Silver and others 2005).

The medial location of the human attention/eye movement region is consistent with a widely held view that the human parietal cortex is organized in a radically different fashion from the macaque and the notion that the human IPL is unique to the species (Glover 2004). The numbers that Brodmann (1909) used to refer to the human IPL were not used in the numerical labeling system he employed when describing an Old World monkey brain. Several anatomical studies, however, have highlighted similarities between human and macaque IPL (Von Bonin and Bailey 1947; Eidelburg and Galaburda 1984). It has been difficult to ascertain the degree of similarity between the IPLs of the two species using functional criteria because the functions of the posterior IPL area, PG, are less well understood. Nevertheless, neurons in the posterior IPL of the macaque are active during the reorienting of attention (Steinmetz and Constantinidis 1995; Constantinidis and Steinmetz 2001), and a region in the human IPL is active when attention or eye

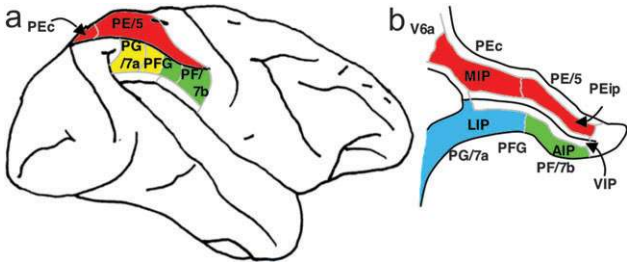

Figure 1. (*a*) The macaque lateral parietal cortex is divided into the IPL and SPL by the IPS. Subdivisions are shown using the terminologies that followed both Brodmann (1909) (e.g., areas 5 and 7) and Von Bonin and Bailey (1947) (PE, PF, PG). (*b*) A large part of the parietal cortex is located in the IPS. The figure summarizes in a diagrammatic form the opened IPS with the AIP at the anterior end of the sulcus on the right. The IPL and SPL are shown below and above the sulcus, respectively. The diagram is based on previous figures (Rushworth and others 1997a; Geyer and others 2000).

movements are redirected (Corbetta and others 2000; Mort, Perry, and others 2003; Thiel and others 2004; Kincade and others 2005).

Rather than looking for functional similarities, the present study used diffusion-weighted imaging (DWI) and probabilistic tractography to examine whether human parietal connectivity patterns resembled those that characterized 3 regions of the macaque IPL and the adjacent lateral IPS. DWI provides information about the orientation of white matter fibers in the brain (Basser and Jones 2002; Beaulieu 2002). Probabilistic tractography is then used to generate estimates of the likelihood of a pathway existing between two brain areas (Behrens, Woolrich, and others 2003; Hagmann and others 2003; Parker and Alexander 2003; Tournier and others 2003). The DWI tractography approach has been used to identify areas of the human thalamus and medial frontal cortex with distinct connectivity patterns (Behrens, Johansen-Berg, and others 2003; Johansen-Berg, Behrens, Robson, and others 2004; Johansen-Berg, Behrens, Sillery, and others 2004). Brain regions distinguished by their DWI tractography profiles are associated with distinct cognitive processes (Johansen-Berg, Behrens, Robson, and others 2004; Johansen-Berg, Behrens, Sillery, and others 2004). Croxson, Johansen-Berg, Behrens, Robson, Pinsk, Gross, and others (2005) have shown that the technique can be used to identify connection patterns in the prefrontal cortices of both macaque and human primates, which resemble those seen in tract-tracing studies in macaques.

The technique has proven particularly robust in identifying the connections of subcortical seed areas in the white matter itself or subcortical nuclei where white matter penetration may be high (Stieltjes and others 2001; Behrens, Johansen-Berg, and others 2003; Johansen-Berg, Behrens, Sillery, and others 2004). Seed areas in the present investigation were therefore the 3 subcortical areas known, in the macaque, to have regionally specific connections with the 3 IPL and lateral IPS regions under investigation. The first seed area was the superior colliculus, which, within the lateral parietal cortex, is most densely connected to the LIP region in the macaque (Lynch and others 1985; Blatt and others 1990; Clower and others 2001; Gaymard and others 2003; Lock and others 2003). The second seed area was the white matter adjacent to the parahippocampal gyrus, which is most densely connected to the posterior IPL region including area PG (Seltzer and Pandya 1984; Cavada and Goldman-Rakic 1989b; Suzuki and Amaral 1994; Lavenex and others 2002). The third region was the third branch of the superior longitudinal fascicle (SLFIII), which is known to carry the projections of the ventral premotor cortex in both the macaque and human brain (Petrides and Pandya 2002; Croxson, Johansen-Berg, Behrens, Robson, Pinsk, Gross, and others 2005). In the macaque, within the parietal cortex, these regions are known to be chiefly interconnected with AIP and the anterior IPL region PF (Matelli and others 1986; Cavada and Goldman-Rakic 1989a).

It is of course the case that each of the 3 IPL and lateral IPS regions is characterized by a number of other anatomical connections. The other connections are less suitable candidates for a DWI tractography study either because the projections pass through areas of crossing fibers, and so cannot be followed reliably by the methods used here, or because, although a connection may have been reported, the white matter course taken by the connection has not been described or depicted. The courses of the connections between the superior colliculus and LIP, between the parahippocampal gyrus and PG, and between the ventral premotor cortex and PF and AIP have all been described in the macaque (Seltzer and Pandya 1984; Petrides and Pandya 2002; Gaymard and others 2003).

Methods

Data Acquisition

We acquired diffusion-weighted data from 9 healthy human subjects (5 male, 4 female, aged 24–35 years) using a 1.5-T Siemens Sonata magnetic resonance scanner with a maximum gradient strength of 40 mT m^{-1}. All subjects gave informed written consent in accordance with ethical approval from the Oxford Research Ethics Committee.

We acquired diffusion-weighted data using echo-planar imaging (72 × 2-mm-thick axial slices, matrix size 128 × 104, field of view 256 × 208 mm^2, giving a voxel size of 2 × 2 × 2 mm). The diffusion weighting was isotropically distributed (Jones and others 1999) along 60 directions using a *b*-value of 1000 s mm^{-2}. For each set of diffusion-weighted data, we acquired 5 volumes with no diffusion weighting at points throughout the sequence. We acquired 3 sets of diffusion-weighted data in total, for subsequent averaging. The total scan time for the DWI protocol was 45 min.

For each subject, we acquired a T_1-weighted anatomical image using a FLASH sequence (TR = 12 ms, TE = 5.65 ms, flip angle = 19°, with elliptical sampling of the *k*-space, giving a voxel size of 1 × 1 × 1 mm in 5.05 min).

Diffusion-Weighted Image Analysis

We corrected diffusion data for eddy currents and head motion using affine registration to a reference volume (Jenkinson and Smith 2001). The data from the 3 acquisitions were subsequently averaged to improve the signal-to-noise ratio.

We performed tissue-type segmentation, skull stripping, and registration on the scans, using tools from the Oxford Centre for Functional Magnetic Resonance Imaging of the Brain's Software Library (www.fmrib.ox.ac.uk/fsl). We performed probabilistic tissue-type segmentation and partial volume estimation on the T_1-weighted image (Zhang and others 2001). We thresholded the results to include only voxels estimated at greater than 35% gray matter and used this to mask the cortical regions. We skull stripped the diffusion- and T_1-weighted images (Smith 2002) and performed affine registration (Jenkinson and Smith 2001) between the first nondiffusion-weighted volume and the T_1-weighted image to derive the transformation matrix between the 2 spaces. We then calculated probability distributions of fiber direction at each voxel using previously described methods (Behrens, Woolrich, and others 2003).

We defined 3 regions for analysis (seed areas) in each subject's left hemisphere according to the anatomical criteria described below. In addition, we defined 6 areas within the parietal cortex (target areas). We transformed the masks into the space of each subject's diffusion data using FLIRT (Jenkinson and Smith 2001) when necessary.

For each subject, we ran probabilistic tractography from all voxels in each seed mask (Behrens, Johansen-Berg, and others 2003; Behrens, Woolrich, and others 2003). From each voxel in the mask, samples were drawn from the connectivity distribution, maintaining knowledge of location in structural and DWI spaces, and we recorded the proportion of these samples that passed through each of the cortical target masks as the probability of connection to that zone.

For each voxel, the number of samples reaching a parietal target area was recorded as a proportion of the total number of samples going to all parietal target areas. For each target area, we then took a mean value for all voxels in the seed area with any connectivity to that target, giving us the mean proportion of projections to each target area. Taking the proportion of projections allows us to compare the projection *patterns* of different seed regions, regardless of the overall probability of connections from different areas that depends on factors such as the overall seed area size. All generated pathways were visually inspected to check for anatomical plausibility prior to intersubject averaging of data.

To determine whether cortical areas possessed characteristic patterns of connection probability from the subcortical areas considered, we carried out repeated-measures analyses of variance on the data, with factors for seed area and target area. Huyhn–Feldt adjustment was applied where necessary.

Definition of Seed Areas

Superior Colliculus

Using the T_1-weighted anatomical image, prior to registration into standard Montreal Neurological Image (MNI) space (Collins and others 1994), masks were drawn over the superior colliculus in the left hemisphere of each subject's brain. An example is shown in Figure 2(*a*). Care was taken to ensure that the mask did not extend into the adjacent midbrain areas. On average, the superior colliculus seed masks were 255-mm^3 voxels in size. Because the focus of the investigation was on the parietal cortical connections, a second more anterior mask ($y = -16$) was used to terminate projections that ran anteriorly through the brachium toward the optic nerve (yellow line Fig. 2*a*). This prevented the connections reaching a region anterior to the thalamus containing a number of other white matter tracts where probabilistic tractography is difficult and "jumping" occurs between the adjacent white matter fiber tracts. Using a simple termination zone, such as the one used here, is desirable because of its simplicity, but it might not be appropriate if the superior collicular connections with frontal areas were to be examined. As can be seen in Results, this precaution did not impede the detection of tracts that run by the pulvinar thalamus to the parietal cortex. The projections from the parietal cortex to the superior colliculus are known to take this route in macaques, and lesions to this area of the human brain affect saccades (Gaymard and others 2003).

Parahippocampal Gyrus

The T_1-weighted anatomical images were transformed into standard MNI space using FLIRT (Jenkinson and Smith 2001), and the parahippocampal gyrus was identified using the criteria outlined by Pruessner and others (2002). In brief, borders of the parahippocampal region were as follows. Its most medial extent was the inferior border of the hippocampus (Fig. 2*b*). The lateral border was at the lateral edge of the collateral sulcus when one collateral sulcus was present but at the

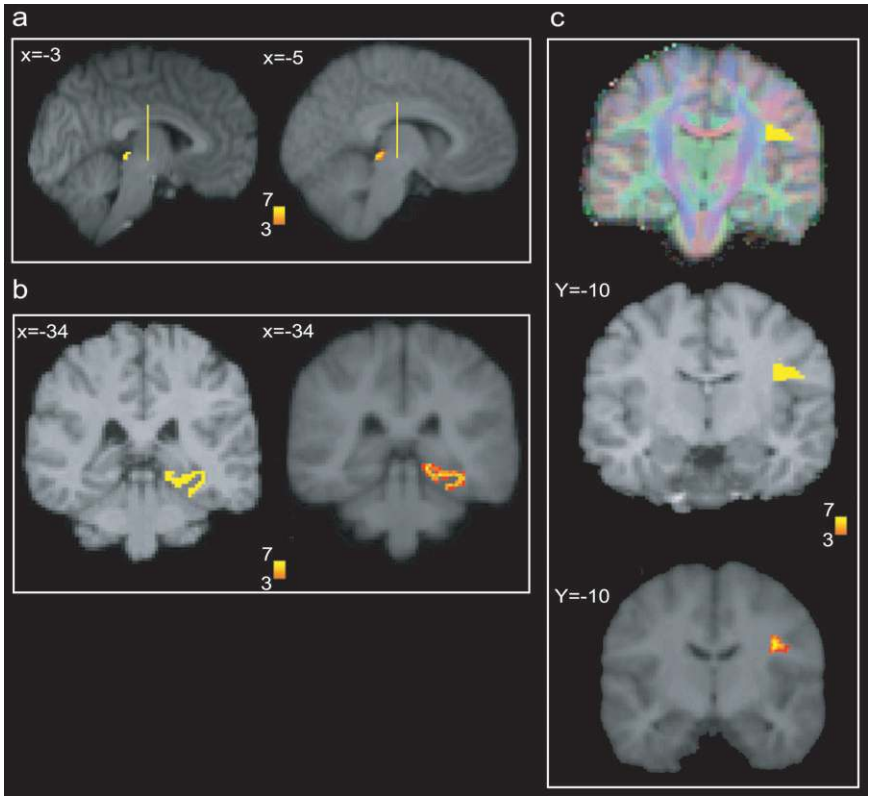

Figure 2. (*a*) An example of the superior colliculus mask superimposed on a sagittal section of the T_1-weighted structural magnetic resonance imaging (MRI) scan for 1 subject after transformation into MNI space (left). Overlap of the superior colliculus masks across subjects superimposed on the group average structural MRI scan is shown on the right. The color scale bar indicates the degree of mask overlap between subjects. At one end of the scale, the red color indicates that a voxel was included in the mask for 3 subjects or more, whereas at the other end, yellow indicates voxel inclusion in the masks of 7 or more subjects. (*b*) An example of the parahippocampal gyrus mask superimposed on a coronal section of the T_1-weighted structural MRI (MNI space) for 1 subject (left). Overlap of the parahippocampal gyrus mask across subjects superimposed on the average structural MRI scan. The scale bar follows the conventions as in 2(*a*). (*c*) An example of the diffusion fractional anisotropy map for 1 subject where red, blue, and green indicate diffusion in a predominantly lateral–medial, dorso-ventral, or anterior–posterior direction. The SLFIII mask is shown in yellow (top). The center of the SLFIII mask is shown superimposed on a coronal section through the same subject's T_1-weighted structural MRI scan after transformation into MNI space (middle). The overlap of the SLFIII mask across subjects is superimposed on the average structural MRI scan. The scale bar follows the same conventions as in 2(*a*,*b*) (bottom).

fundus of the more lateral collateral sulcus when two collateral sulci were present. Its anterior border was 5 mm posterior to the disappearance of the gyrus intralimbicus, whereas its posterior border was at the same level as the last appearance of the hippocampus inferomedial to the trigone of the lateral ventricle. Because diffusion anisotropy was expected to be low in the parahippocampal cortex itself, the seed area was placed in the immediately adjacent white matter (Fig. 2*b*). The masks were, on average, 2654 mm^3 in size.

In the macaque, the parahippocampal gyrus is known to project to the posterior IPL via 2 routes (Seltzer and Pandya 1984). Some projections are carried in a medial route via the cingulum bundle. In the macaque, the cingulum bundle conveys not only the connections of the posterior IPL but also the connections of widespread retrosplenial, medial parietal, and cingulate areas with several thalamic, premotor, and prefrontal regions (Mufson and Pandya 1984). The limited spatial resolution of the DWI and tractography approach means that it is not possible to identify the projections between the parahippocampal gyrus and posterior IPL among the many other projections to medial cortical regions.

The present study therefore focused on the second route that interconnects the parahippocampal gyrus and IPL—the inferior longitudinal fascicle (ILF). The ILF connections run laterally adjacent to the optic radiations in the geniculocalcarine tract. Because ILF connections between the parahippocampal gyrus and posterior IPL do not substantially cross the optic radiations, it is possible to distinguish them from the thalamic connections with posterior visual cortical areas even with DWI tractography if care is taken. The optic radiations move in a predominantly anterior-to-posterior direction, but on leaving the thalamus, they initially bow laterally before turning back medially to reach the medial visual areas. By only considering projections that emerged either superior to the $z = 10$ plane and lateral to the $x = -28$ plane or posterior to the $y = -70$ plane and lateral to the $x = -28$ plane, it was possible to exclude the medial projections from the parahippocampal gyrus running in the cingulum bundle and the medial and inferior projections running in the optic radiations and to focus on the parahippocampal projections running in the ILF. Results, however, presents tractography from the parahippocampal gyrus both before and after these additional constraints were imposed.

SLFIII and the Ventral Premotor

The parietal connections of the ventral premotor cortex were examined by analyzing the parietal connections of SLFIII. This approach was taken for several reasons. First, the posterior projections of the ventral premotor region are known to be conveyed via SLFIII in both humans and macaques (Petrides and Pandya 2002; Croxson, Johansen-Berg, Behrens, Robson, Pinsk, Gross, and others 2005). Second, the position of SLFIII is now well characterized in the human brain (Mori and others 2002; Croxson, Johansen-Berg, Behrens, Robson, Pinsk, Gross, and others 2005; Makris and others 2005). Third, such an approach avoided having to impose additional constraints on which connection paths were considered, as was the case for the parahippocampal gyrus.

Each individual subject's diffusion anisotropy map was used to delineate a region of high anterior–posterior diffusion dorsolateral to the putamen, which has previously been shown to correspond to SLFIII (Croxson, Johansen-Berg, Behrens, Robson, Pinsk, Gross, and others 2005; Makris and others 2005). The seed mask occupied 5 adjacent coronal sections, and the central section was in the same coronal section as the anterior and ventral central sulcus close to the premotor cortex (Fig. 2*c*). On average, the masks were 948 mm^3 in size.

Definition of Target Areas

The parietal cortex was divided into 6 regions. Because the focus of the investigation was on identifying brain regions with connections that resembled those of macaque IPL and lateral IPS, the target areas were on the lateral surface of the parietal lobe and the medial surface was not investigated. Because of the possibility that areas resembling the macaque IPL are found in the SPL and medial IPS of the human brain, these areas were also included in the investigation. In brief, the IPL was divided into a posterior and an anterior target region, the SPL was divided into, first, a lateral and posterior target region that also included the adjacent medial IPS and, second, a more medial and anterior division. The final 2 regions were positioned on either side of the descending segment of the IPS. Figure 3(*a–e*) shows the regions of between-subject overlap in the 6 target masks superimposed on the group average magnetic resonance imaging scan. Figure 3(*f-j*) shows an example of the division into 6 areas in 1 subject.

Anterior IPS and Anterior IPL (AIPL)

A single mask, referred to as the AIPL, covered both the anterior IPS and the anterior IPL. The mask included the IPS and supramarginal gyrus tissue anterior to Jensen's sulcus and the ascending IPS or posterior bank of the postcentral sulcus (green area, Fig. 3*e,j*). The medial boundary of the AIPL was the depth of the IPS (Fig. 3*a,f*). The lateral boundary was the lateral fissure/superior temporal gyrus (Fig. 3*a,f*). Across the group, the region of AIPL overlap for 3 or more subjects extended from $x = -34$ to $x = -66$, $y = -55$ to $y = -26$, $z = 57$ to $z = 78$.

It might be possible to dissociate the anterior IPS and IPL regions in future studies, but the resolution of DWI and tractography currently make it difficult to distinguish their connection patterns with ventral premotor cortical regions.

Angular Gyrus (ANG)

An angular gyrus mask (ANG) covered the IPL posterior to Jensen's sulcus and extended posteriorly and ventrally to the superior bank of the horizontal branch of the superior temporal sulcus (yellow area, Fig. 3*e,j*). Tissue deep within the superior temporal sulcus was not included. Medially, the mask included a small amount of tissue in the immediately adjacent lateral bank of the horizontal segment of the IPS (Fig. 3*b,g*). In posterior coronal sections, the horizontal segment of the IPS gives way to the much deeper descending segment of the IPS, and a separate mask was used to cover the lateral bank of the descending segment of the IPS at this point (white area in Fig. 3*g*). Across the group, the region of ANG overlap for 3 or more subjects extended from $x = -28$ to $x = -59$, $y = -91$ to $y = -55$, $z = 20$ to $z = 60$.

First Superior Parietal Lobule Region (SPL1)

The anterior border of the first SPL (SPL1) mask was a line extending from the inferior postcentral sulcus that ran parallel with the central sulcus toward the level of the marginal ramus of the cingulate sulcus on the medial surface (red area in Fig. 3*c,h*). In some subjects, a superior postcentral sulcus was present and the anterior boundary partly overlapped with the ascending portion of this sulcus. The medial boundary was approximately 5 mm from the medial surface (Fig. 3*a,f*). Posteriorly and laterally, the mask extended to the transverse sulcus of the SPL (Fig. 3*a,f*). The transverse sulcus is a small sulcus that runs from an anterior and lateral position to a posterior and medial position within the SPL medial and approximately parallel to the main branch of the IPS (Duvernoy 1991). When the transverse parietal sulcus was unclear, an axial section was used to place the posterior and lateral boundary halfway between the medial bank of the IPS and the marginal ramus of the cingulate sulcus along a line parallel to the main branch of the IPS. Across the group, the region of SPL1 overlap for 3 or more subjects extended from $x = -8$ to $x = -30$, $y = -57$ to $y = -39$, $z = 57$ to $z = 78$.

Second Superior Parietal Lobule Region (SPL2)

A second mask (SPL2) covered the remaining division of the SPL lateral and posterior to the transverse sulcus and included the adjacent medial wall of the IPS. The medial and anterior boundary was based on the position of the transverse parietal sulcus as described for SPL1 (light blue, Fig. 3*a,f*). The posterior and lateral boundary was the depth of the horizontal segment of the IPS (Fig. 3*a,f*). A separate mask covered the tissue on the medial bank of the descending IPS (dark blue, Fig. 3*b,g*). Across the group, the region of SPL2 overlap for 3 or more subjects extended from $x = -14$ to $x = -40$, $y = -76$ to $y = -44$, $z = 40$ to $z = 71$.

Medial Descending IPS (IPSdm)

Separate masks were used to cover the banks of the most posterior part of the IPS—the descending segment of the IPS. Moving posteriorly through coronal sections, the descending IPS is readily distinguished usually appearing first either as a separate sulcus medial to the main horizontal branch of the IPS or as a medially projecting branch of the

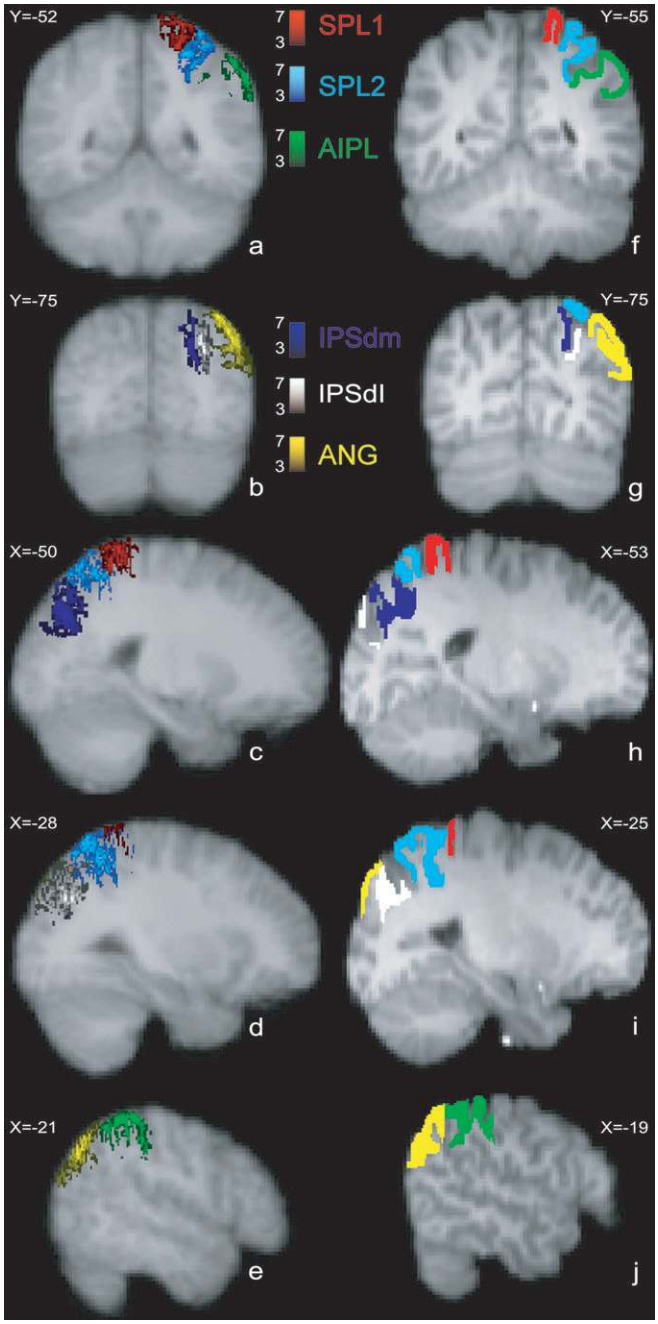

Figure 3. (*a*) Overlap of the 3 more anterior parietal target masks, anterior IPL and the adjacent anterior IPS (AIPL), medial SPL (SPL1), and lateral SPL (SPL2), across subjects superimposed on a coronal section of the group average magnetic resonance imaging (MRI) scan. The scale bars indicate the degree of overlap using the conventions established in previous figures. (*b*) Overlap of the 3 more posterior parietal target masks, angular gyrus (ANG), medial bank of the descending IPS (IPSdm), and lateral bank of the descending IPS (IPSdl), on a coronal section of the group average MRI scan. Overlap of the most medial regions, SPL1, SPL2, IPSdm (*c*), regions in a relatively central sagittal plane, SPL2, IPSdl (*d*), and the most lateral regions, AIPL and ANG, are shown on sagittal sections through the group average MRI scan. (*f*) An example of the 3 more anterior parietal target masks, AIPL, SPL1, and SPL2, in a single subject superimposed on the T_1-weighted structural MRI scan after transformation into MNI space. The coronal section is the most posterior one to include the AIPL region in this subject. (*g*) An example of the 3 more posterior parietal target masks, ANG, IPSdm, and IPSdl, in the same single subject. Examples of the most medial regions, SPL1, SPL2, IPSdm (*c*), regions in a relatively central sagittal plane, SPL2, IPSdl (*d*), and the most lateral regions, AIPL and ANG, are shown on sagittal sections of the same individual's MRI scan.

horizontal IPS (Fig. 3*g*). One mask was used to cover the medial bank of the descending IPS (IPSdm). The IPSdm extended ventrally to the depth of the IPS or, more posteriorly, the transverse occipital sulcus (dark blue, Fig. 3*b*,*g*). It extended dorsally to the lip of the IPS (Fig. 3*b*,*g*). Posteriorly, the IPSdm extended to the last coronal slice on which the IPS was still visible (Fig. 3*c*,*b*). Across the group, the region of IPSdm overlap for 3 or more subjects extended from $x = -14$ to $x = -27$, $y = -87$ to $y = -63$, $z = 20$ to $z = 56$.

Lateral Descending IPS (IPSdl)

A separate mask covered the lateral bank of the descending segment of the IPS (IPSdl). The IPSdl extended ventrally to the depth of the IPS or, more posteriorly, to the transverse occipital sulcus (white area, Fig. 3*b*,*g*). It extended dorsally to the lip of the IPS (Fig. 3*b*,*g*). Posteriorly, the IPSdl extended to the last coronal slice on which the IPS was still visible (Fig. 3*c*,*b*). Across the group, the region of IPSdl overlap for 3 or more subjects extended from $x = -24$ to $x = -32$, $y = -86$ to $y = -64$, $z = 20$ to $z = 49$.

Results

The 3 seed regions, superior colliculus, parahippocampal gyrus, and SLFIII, had distinct connection probabilities with the 6 parietal regions ($F = 19.484$, df = 10,80, $P < 0.001$). The connection probabilities of each area are summarized in the figures showing the group connection paths and a histogram of the group connection probabilities with each of the 6 parietal seed areas (Figs. 4–6).

Superior Colliculus

Across subjects, the tractography analysis consistently identified an approximately ventrodorsally oriented pathway by the pulvinar thalamus and adjacent posterior limb of the internal capsule (Fig. 4*a*). Across all subjects, the pathway continued dorsally to the parietal cortex, and within the parietal cortex, the highest probability of connection was with the lateral and posterior SPL (Fig. 4*b*,*c*). Quantitative analysis revealed significant differences in the probabilities of connections between superior colliculus and the 6 parietal regions ($F = 6.123$, df = 5,40, $P = 0.001$) with the highest probability in the SPL2 region that covered the lateral and posterior portion of the SPL and the adjacent medial bank of the IPS (Fig. 4*d*).

Parahippocampal Gyrus

Across subjects, the tractography analysis consistently identified a pathway with a ventral–anterior to dorsal–posterior orientation within the lateral temporal lobe and the most posterior part of the parietal cortex that appeared to correspond to part of the ILF. As explained in Methods, 2 analyses were performed. In the second analysis, only those projections that emerged dorsal to an axial plane at $z = 10$ and lateral to $x = -28$ or posterior to a coronal plane at $y = -70$ and lateral to $x = -28$ were considered. The restrictions meant that it was possible to focus on the connections of the ILF in the absence of labeling of the two other fiber bundles—more medial projections of the parahippocampal gyrus via the cingulum bundle or the more medial and ventral projections of the optic radiations. Regardless of whether these restrictions were applied, the only region in the lateral parietal cortex with a high probability of connection with the parahippocampal gyrus was a posterior and ventral portion of the angular gyrus (Fig. 5*a*,*b*). It was noticeable that the region of high-connection probability extended onto the adjacent superior occipital gyrus. The same region of high-connection probability in the posterior and ventral angular

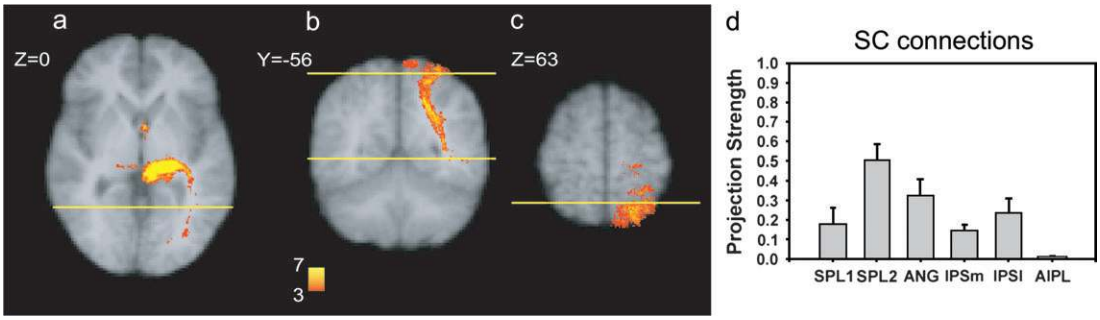

Figure 4. Overlap of the superior colliculus projection pathway across subjects superimposed on the group average of the T_1-weighted structural magnetic resonance imaging scans following transformation into MNI space. Each subject's tract was binarized so that all areas with an above-zero probability of connection to the superior colliculus were assigned a value of 1. The tracts were then summed together across subjects. The scale bar indicates the degree of overlap using the conventions established in previous figures; at one end of the scale, the red color indicates that a voxel was included in the mask for 3 subjects or more, whereas at the other end, yellow indicates voxel inclusion in the masks of 7 or more subjects. (*a*) An axial section shows the projection emerging by the pulvinar thalamus and the adjacent posterior limb of the internal capsule. (*b*) The main pathway to the medial IPS on a coronal section. (*c*) An axial section illustrates that within the SPL the projection zone was predominantly lateral and posterior. (*d*) Results of quantitative tractography to the 6 parietal regions averaged across subjects. The highest probability projection zone was largely included within the SPL2 that occupied the lateral and posterior part of the SPL and extended onto the medial wall of the IPS.

gyrus and the adjacent superior occipital gyrus was observed after exclusion of the cingulum bundle and optic radiation projections, but the picture was not confused by the presence of high-probability optic radiation connections to the medial occipital cortex or a high probability of cingulum connections to other medial surface areas (Fig. 5*c*,*d*). Quantitative analysis revealed significant differences in the connection probabilities with the 6 parietal targets ($F = 10.142$, df = 5,40, $P < 0.001$) with the highest probability in the ANG region (Fig. 5*e*). A comparison of Figures 4 and 5 shows that there was some overlap between the probabilistic connection patterns of the superior colliculus and the parahippocampal gyrus. Nevertheless, the superior colliculus connection probabilities were centered on a more dorsal and medial region in the SPL2, whereas the parahippocampal projections were centered on a more lateral and ventral region in the ANG. The connection probability patterns of the 2 seed areas were significantly different ($F = 4.809$, df = 5,40, $P = 0.005$).

SLFIII and Ventral Premotor Cortex

Across subjects, the tractography analysis consistently identified a pathway resembling the SLFIII that extended anteriorly into the frontal lobe with a high probability of connection to the ventral premotor and the adjacent pars opercularis (Fig. 6*a*,*b*). Within the parietal cortex, the highest probability of connection was with the supramarginal gyrus of the anterior IPL and the adjacent anterior IPS, although in some cases the region of high-connection probability extended posteriorly in the anterior ANG (Fig. 6*c*). Quantitative analysis confirmed that there were significant differences in connection probabilities between the SLFIII with the 6 parietal regions ($F = 32.559$, df = 5,40, $P < 0.001$) with the highest connection probability in the AIPL region that contained the supramarginal gyrus and the adjacent anterior IPS region. The pattern of connection probabilities was significantly different from that seen for either the superior colliculus ($F = 25.002$, df = 5,40, $P < 0.001$) or the parahippocampal gyrus ($F = 27.734$, df = 5,40, $P < 0.001$).

Discussion

Probabilistic diffusion tractography suggested that 3 regions of human parietal cortex were distinguished by their patterns of connections with the superior colliculus, parahippocampal gyrus, and ventral premotor cortex via the SLFIII. In the macaque, connections with these 3 regions distinguish 3 divisions of the IPL and the adjacent lateral IPS. In the macaque, the ventral premotor cortex is connected with the anterior IPL region PF and with area AIP in the adjacent IPS (Matelli and others 1986; Cavada and Goldman-Rakic 1989a). In the macaque, the parahippocampal cortex is connected with the more posterior IPL including areas PG and Opt (Seltzer and Pandya 1984; Cavada and Goldman-Rakic 1989b; Suzuki and Amaral 1994; Lavenex and others 2002). Although there is some spread of parahippocampal connections to LIP in the adjacent posterior IPS, the amount is less than in the neighboring PG. By contrast, the superior colliculus has stronger connections with the LIP region in the posterior IPS than with the posterior IPL areas (Lynch and others 1985; Andersen and others 1990; Clower and others 2001; Gaymard and others 2003).

Connections with Superior Colliculus

In the present study, the superior colliculus high-probability connection pathway to the parietal cortex traveled in the vicinity of the pulvinar thalamus and posterior internal capsule (Fig. 4*a*). Connections from the superior colliculus are known to pass by a similar route in the macaque (Benevento and Fallon 1975; Bender and Baizer 1984; Gaymard and others 2003), and pulvinar lesions disrupt eye movements if they affect the connections running between the cortex and the superior colliculus (Bender and Baizer 1990). There is suggestive evidence that a similar route is taken by fibers in the human brain; lesions in the posterior internal capsule disrupt eye movements in patients (Gaymard and others 2003).

The medial IPS region contained within the SPL2 mask was the parietal region with the highest probability of connection with the superior colliculus (Fig. 4*b*,*c*,*d*). It is difficult to use DWI tractography to compare the connection probabilities of 1 structure with several target structures that are all distant from one another because the connection probabilities for each target may be affected by different artifacts. For example, crossing fibers or a ventricle may be close to the connections of 1 target area, but they may be distant from the connections of another target area. The present study therefore focused just on

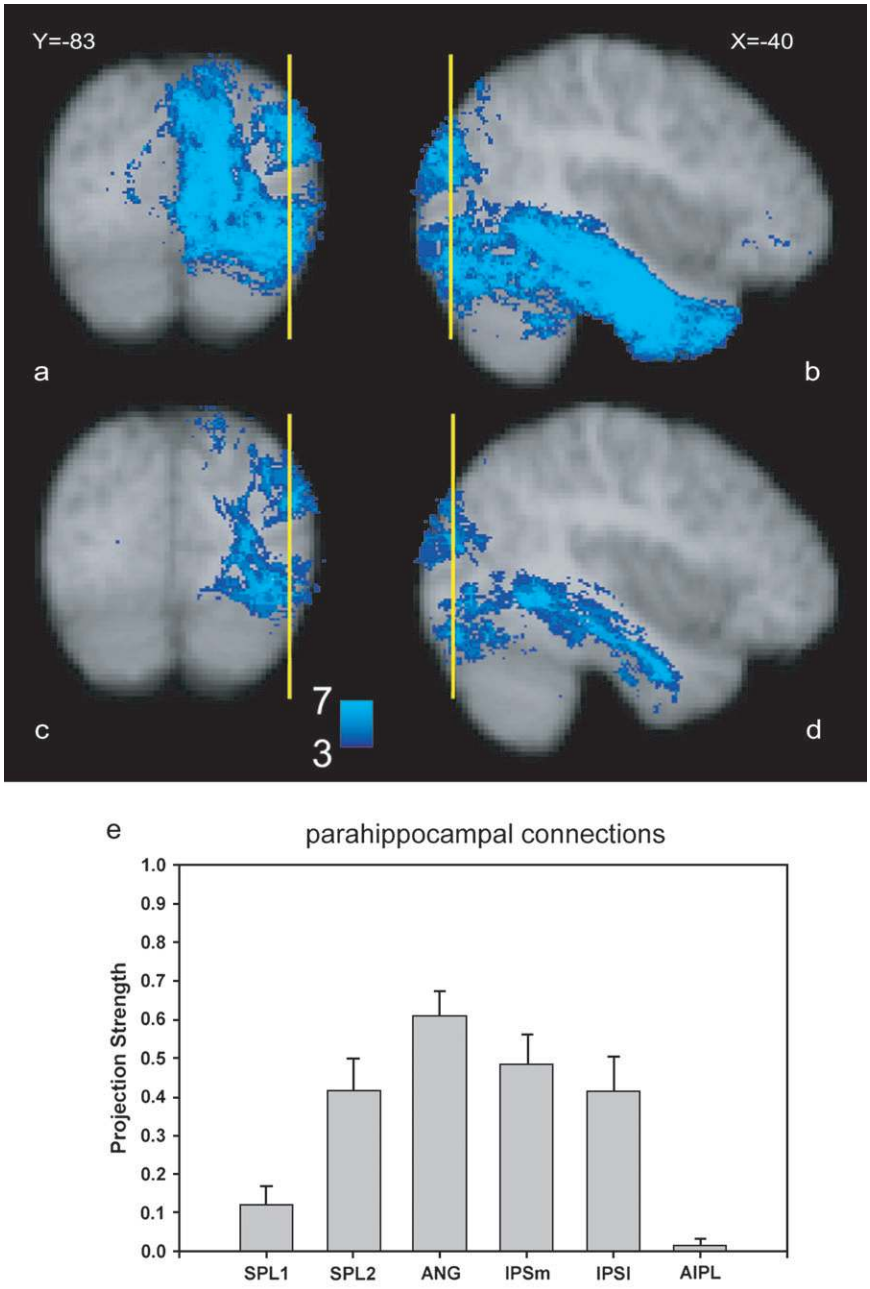

Figure 5. Overlap of the parahippocampal projection pathway across subjects superimposed on the group average of the T_1-weighted structural magnetic resonance imaging scans following transformation into MNI space. The scale bar indicates the degree of overlap using the conventions established in previous figures. (*a*) A sagittal section illustrates how, in the absence of any exclusion criteria during tracking, a high-probability connection region was seen in only 1 lateral parietal region in the posterior part of the angular gyrus and extending to the superior occipital gyrus. The projection pathway included a lateral division that resembled the ILF and also a more medial pathway in the cingulum bundle and a contamination by geniculocalcarine projections in the adjacent optic radiations that resulted in the highlighting of connection pathways to retrosplenial, cingulate, and medial occipital regions, respectively (*b*). It was, however, possible to isolate the parahippocampal projections via the ILF and still find a high-probability connection area in the angular gyrus and superior occipital gyrus (*c*,*d*). (*e*) Results of quantitative tractography to the 6 parietal regions averaged across subjects. The highest probability projection zone included the ANG mask that occupied the posterior IPL.

the connections of the adjacent parietal areas to ensure that any biases affected estimates of connection probabilities in similar ways for all the areas considered.

In the macaque, the parietal cortex is known to consist of a number of specialized subfields that are concerned with both eye and arm movements and receive somatosensory, auditory, and visual inputs (Colby and Goldberg 1999; Andersen and Buneo 2002). In the cat, there is evidence that certain somatosensory areas, such as the fourth somatosensory cortical area, SIV, project to the superior colliculus (Clemo and Stein 1983; Wallace and others 1993). Within the parietal cortex of the macaque, however, it is area LIP, an area dominated by vision and principally concerned with eye movements, that is most strongly connected with the superior colliculus (Lynch and others 1985; Clower and others 2001; Lock and others 2003).

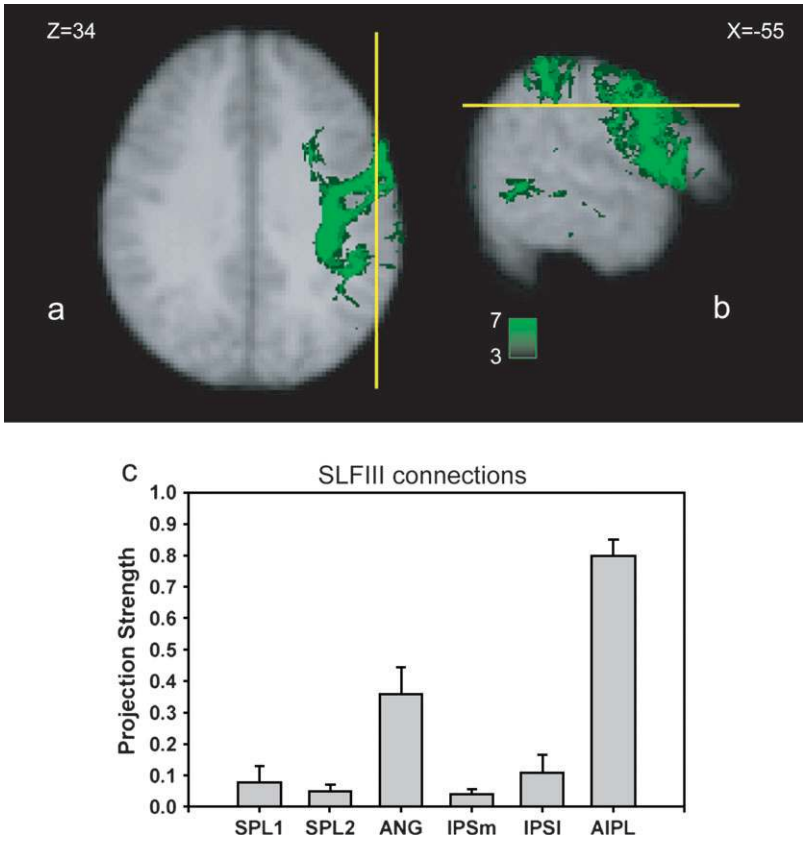

Figure 6. Overlap of the SLFIII projection pathway across subjects superimposed on the group average of the T_1-weighted structural magnetic resonance imaging scans following transformation into MNI space. The scale bar indicates the degree of overlap using the conventions established in previous figures. (*a*) An axial section illustrates the path of the SLFIII running from ventral premotor and the adjacent pars opercularis toward the anterior IPL. (*b*) Sagittal sections through the region of high-connection probability in the supramarginal gyrus of the IPL and adjacent IPS. (*c*) Results of quantitative tractography to the 6 parietal regions averaged across subjects. The highest probability projection zone was the AIPL mask that included the supramarginal gyrus in the anterior IPL and the adjacent anterior IPS. The second highest probability projection zone was the angular gyrus region, ANG, in the posterior IPL. Unlike the parahippocampal connections with posterior ANG, the connections mediated by the SLFIII were with the more anterior and dorsal ANG.

Because some connections between the parietal cortex and the superior colliculus may run within the lateral part of the pulvinar thalamus, it is possible that the probabilistic DWI approach also picked up some connections between the pulvinar itself and the parietal cortex. In the macaque, the cells of the lateral pulvinar, however, also project more strongly to area LIP than they do to other adjacent parietal areas (Hardy and Lynch 1992).

The superior colliculus is closely involved in the control of eye movements. The SPL2 region with the highest probability of connection with the superior colliculus lies adjacent to a superior part of the medial bank of the IPS identified with covert orienting of the visuospatial attention and with overt movements of the eyes in functional imaging studies. Figure 7(*b*) shows the position Grosbras and others (2005) identified, on the basis of a meta-analysis of more than 40 studies, as likely to be activated when subjects were performing a covert attention task. It is close to peaks emphasized by Gitelman and others (1999) and shown to have some degree of retinotopic mapping for saccades (Sereno and others 2001). Also shown in Figure 7(*b*) are data from 2 studies that have compared reflexive orienting and saccades with activation recording during reorienting or during redirecting of saccades (Mort, Perry, and others 2003; Kincade and others 2005). Activations for reflexive orienting and saccade generation are in or close to the region identified here as having a high probability of connection with the superior colliculus. In some cases, activation peaks do not completely overlap with the region identified as having a high probability of connection to the superior colliculus, but it should be remembered that normally the full region of suprathreshold activation in a neuroimaging study extends beyond the activation peak. Moreover, some slight degree of separation between activation areas and high-probability connection zones might be expected if fMRI studies of brain activation and diffusion tractography studies of brain connection are not equally susceptible to identical artifacts.

It was noted that the high-probability connection region included a swathe of tissue extending ventrally along the medial bank of the IPS. Figure 7(*a*) shows that, more ventrally, the high-probability connection region was adjacent to the anterior limit of the descending IPS in the vicinity of a more ventral region that was also highly likely to be activated in the meta-analysis (Grosbras and others 2005). Several studies have emphasized activation in this location and have referred to it as either the ventral IPS or the intraparietal/transverse occipital region (Corbetta and others 1998, 2000; Kincade and others 2005). Activation in this region can be clearly dissociated from more dorsomedial activations linked to limb movement intentions (Rushworth, Paus, and Sipila 2001). Retinotopically mapped regions in which activation is modulated by attention but not by visual stimulation are situated between the more ventral and dorsal IPS regions (Silver and others 2005). Whether 1 or more

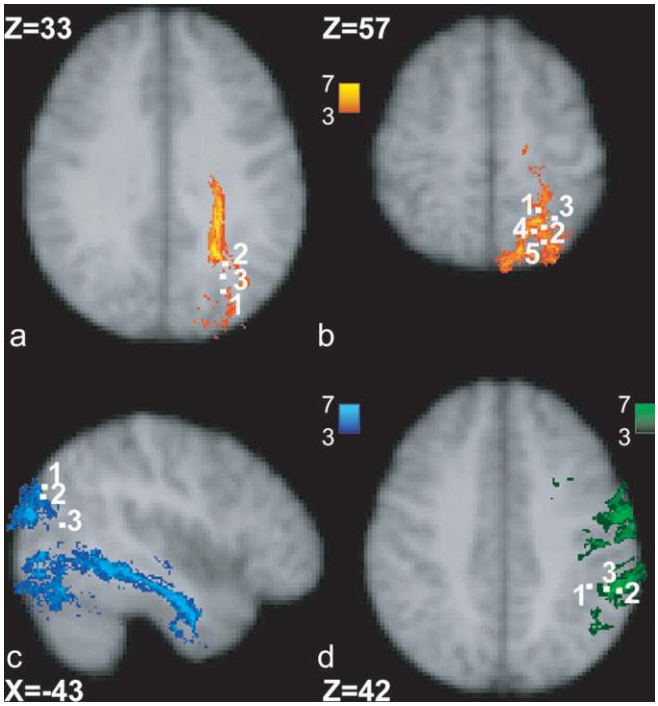

Figure 7. The parietal regions with a high probability of connection to the superior colliculus, parahippocampal, and ventral premotor cortex are associated with activations recorded in distinct types of cognitive task. (*a*) The superior colliculus pathway passed anterior and adjacent to the descending branch of the IPS and a region described as either ventral IPS or IPS/transverse occipital sulcus boundary. Activations in this region have been related to visuospatial attention and eye movement (1. Grosbras and others 2005). They are more closely associated with attentional preparation than with reorienting to salient stimuli (2. Kincade and others 2005) or motor intentions (3. Rushworth, Paus, and Sipila 2001). The *x* and *y* coordinates are plotted on the axial plane at $z = 33$. (*b*) The superior colliculus high-probability connection region extended to the more dorsal medial IPS where activations have also been related to visuospatial attention and eye movements (1. Gitelman and others 1999, 2. Grosbras and others 2005). The area may be retinotopically mapped (3. Sereno and others 2001) and more concerned with directed attention or eye movements than with redirected attention or eye movements (4. Mort, Perry, and others 2003, 5. Kincade and others 2005). The *x* and *y* coordinates are plotted on the axial plane at $z = 57$. (*c*) The angular gyrus that is more likely to be connected to the parahippocampal gyrus is more closely associated with the redirecting of attention or eye movements (1. Mort, Perry, and others 2003, 2. Thiel and others 2004, 3. Kincade and others 2005). The *y* and *z* coordinates are plotted on the sagittal slice at $x = -43$. (*d*) The ventral premotor cortex high-probability connection region in the anterior and lateral IPS is associated with visually guided grasping and visuotactile matching (1. Both Binkofski, Buccino, Posse, and others 1999 and Grefkes and others 2002, 2. Shikata and others 2003) and covert intended hand movements as opposed to covert visuospatial attention (3. Rushworth, Paus, and Sipila 2001). The *x* and *y* coordinates are plotted on axial slice at $z = 42$.

of these regions most resembles the macaque LIP region is currently debated. It is known that brain areas may duplicate during speciation, so there may be more than 1 human IPS region with a functional resemblance to macaque LIP (Sereno and Tootell 2005).

It is important to note that the parietal cortex is not the only cortical region connected with the superior colliculi and that the superior colliculi are not the only subcortical targets of parietal connections. In several primate species, when retrograde tracers are injected into the superior colliculus, labeled cells are found throughout many striate, prestriate, and frontal areas (Fries 1984; Lock and others 2003; Collins and others 2005). The same is likely to be true in the human brain; there is a suggestion of some connections traveling toward prestriate and striate areas in Figure 4(*a*). The connection strength for the striate and prestriate areas appears to be lower, but this may just be a consequence of the proximity of other fibers in the geniculocalacarine tract. The absence of frontal connections in the present study is due to the placement of a mask anterior to the superior colliculus (Fig. 2*a*) to prevent tracks traveling toward the optic nerve and toward a region of high diffusion anisotropy anterior to the thalamus where jumping of connectivity between adjacent tracts appears to occur.

The superior colliculus is not the only subcortical region with which the parietal cortex is connected; there are connections to the basal ganglia and to the cerebellum via the pons (Glickstein 2003). Parietal regions in the macaque are not just distinguished by the patterns of their connections with the superior colliculus but by the pattern of their connections with each of these areas. It will be important for future studies to examine whether the distribution of these other connections can also be used to confirm the identity of areas in the human parietal cortex.

Connections with the Parahippocampal Gyrus

There was a high probability of connection between the parahippocampal gyrus and the angular gyrus in the posterior IPL, and this can be seen most clearly in Figure 5(*c–e*). The high-probability connection included the most posterior angular gyrus between the horizontal and vertical branches of the superior temporal sulcus and extended ventrally to include part of the adjacent superior occipital gyrus. The connection path ran lateral to the hippocampus and medial to the lateral surface of the temporal lobe in a posterior dorsal direction (Fig. 5*d*). The connection path also extended anteriorly into the anterior temporal lobe (Fig. 5*d*). In terms of its position and connections, the path resembles the ILF in the macaque (Seltzer and Pandya 1984).

Whereas Figure 5(*c,d*) shows the connection probabilities when the ILF route is isolated, Figure 5(*a,b*) shows the connection probabilities when 1) a medial connection route is also considered and 2) the ILF route is contaminated by contact with the adjacent optic radiations. As in the monkey (Seltzer and Pandya 1986), connections between the parietal cortex and the medial temporal lobe also travel via a medial route in or adjacent to the cingulum bundle. The limited spatial resolution of human DWI tractography meant that, after intermixing, the fibers became indistinguishable from those connecting to an extensive region on the medial surface including cingulate and retrosplenial areas (Mufson and Pandya 1984). Again, as in the monkey (Seltzer and Pandya 1984), the ILF route in our subjects passed close to the optic radiations as they bowed laterally in Meyer's loop. The optic radiations in turn have a high probability of connection to the visual cortex in the medial occipital lobe (Fig. 5*a,b*, Behrens, Johansen-Berg, and others 2003). Even though inclusion of cingulum and optic radiation connections alongside the lateral ILF connections in Figure 5(*a,b*) produces a more confusing picture, it is still clear that the angular gyrus is the only lateral parietal region with a significant probability of connection to the parahippocampal gyrus. This is not surprising because, among lateral parietal areas, even the medial cingulum route between the medial temporal lobe and the parietal cortex only projects to the posterior IPL areas PG and Opt (Seltzer and Pandya 1984) and the optic radiation projections mostly terminate outside the parietal lobe. The lateral ILF pathway to the parietal lobe can, nevertheless, be isolated (Fig. 5*c,d*) because it runs more dorsal ($z > 10$ mm) and because, for most of its course, it is more lateral

than the optic radiations and because it is more lateral than the cingulum route ($x < -28$ mm) in all subjects.

The angular gyrus and superior occipital gyrus areas that have a high probability of connection to the parahippocampal cortex have not been closely identified with attention orienting in imaging studies. Activations are recorded in this region when subjects redirect saccades or reorient attention (Mort, Perry, and others 2003; Thiel and others 2004, 2005; Kincade and others 2005). Figure 7(*c*) shows activations recorded in 3 studies that compared trials on which subjects reoriented the direction of attention or saccades with trials where the required direction of attention or saccades remained constant. Activation decreases in this area with attentional priming (Devlin and others 2004). Transcranial magnetic stimulation at a similar location disrupts the reorienting of attention (Rushworth, Ellison, and Walsh 2001) and lesions that lead to neglect overlap in this region (Mort, Malhotra, and others 2003). The human posterior IPL therefore has some functional similarities with the macaque posterior IPL. Neurons in the macaque posterior IPL decrease their activity with repeated presentation of a stimulus at the same location and increase their activity when attention must be reoriented (Steinmetz and Constantinidis 1995; Constantinidis and Steinmetz 2001). Lesions in this region disrupt aspects of visual attention (Lawler and Cowey 1987; Lynch and McLaren 1989). Corbetta and Shulman (2002) have argued for a dissociation between a more dorsal system centered on the IPS that is concerned with preparation and attention and a more ventral system that includes the IPL that is concerned with reorienting to salient events. The distinctive connection patterns of the superior colliculus and parahippocampal gyrus with the IPS and angular gyrus may contribute to the functional specializations of the 2 regions. Interestingly, Mort, Malhotra, and others (2003) found, in addition to the angular gyrus, a second focus for neglect-causing lesions that was centered within a few millimeters of the parahippocampal seed region used in the present study.

Connections with the Ventral Premotor Cortex

In the macaque, the SLFIII mediates the connections of the ventral premotor cortex (Petrides and Pandya 2002), and DWI tractography has shown that the same is true in the human brain (Croxson, Johansen-Berg, Behrens, Robson, Pinsk, Gross, and others 2005). Figure 6(*a*,*b*) illustrates connections with the ventral premotor region extending into the pars opercularis of the ventral prefrontal cortex. Within the parietal cortex, the highest probability of connection was in the anterior IPL and the adjacent anterior IPS regions (Fig. 6*c*). The high-probability connection region included or was adjacent to a human parietal region with functional resemblances to the macaque AIP (Fig.7*d*). Activation peaks have been recorded here when grasping movements are made and during visuotactile matching, and in addition, lesions disrupt grasping movements (Binkofski and others 1998; Binkofski, Buccino, Posse, and others 1999; Binkofski, Buccino, Stephan, and others 1999; de Jong and others 2001; Grefkes and others 2002). The region is also active in motor intention tasks that require covert preparation of hand movements rather than covert visuospatial orienting (Rushworth, Krams, and others 2001). Neurons are active in the macaque IPL and the adjacent AIP when grasping movements are made (Sakata and others 1999). In the macaque, lesions disrupt aspects of forelimb movement control but leave visuospatial processes unaffected (Rushworth and others 1997b, 1998).

Conclusions

DWI tractography is limited in comparison with tracer injection techniques that can be used in nonhuman animals. It can neither identify the direction of connections nor the lamination termination pattern. In some instances, it has proved difficult to directly track connections between cortical regions, but it has proved possible to use probabilistic tractography to provide a quantitative estimate of connection probability between subcortical nuclei or white matter regions, where the fractional anisotropy of the diffusion signal is high, and the cortex (Stieltjes and others 2001; Behrens, Johansen-Berg, and others 2003; Johansen-Berg, Behrens, Sillery, and others 2004; Lehericy and others 2004). It is also difficult to follow projections through regions of fiber crossing, although this may be ameliorated by scanning at higher spatial resolutions and using more advanced modeling techniques (Parker and Alexander 2003; Tuch and others 2003). Importantly, however, DWI and probabilistic tractography can be used to demonstrate the relevance of the detailed neurophysiological and anatomical studies that are only possible in nonhuman animals for understanding of human brain function.

In summary, the connection patterns with the superior colliculus, parahippocampal gyrus, and ventral premotor cortex, which distinguish 3 regions of the macaque IPL and IPS, distinguish 3 regions of the human parietal cortex (Fig. 8). In 2 cases, parahippocampal gyrus and ventral premotor cortex,

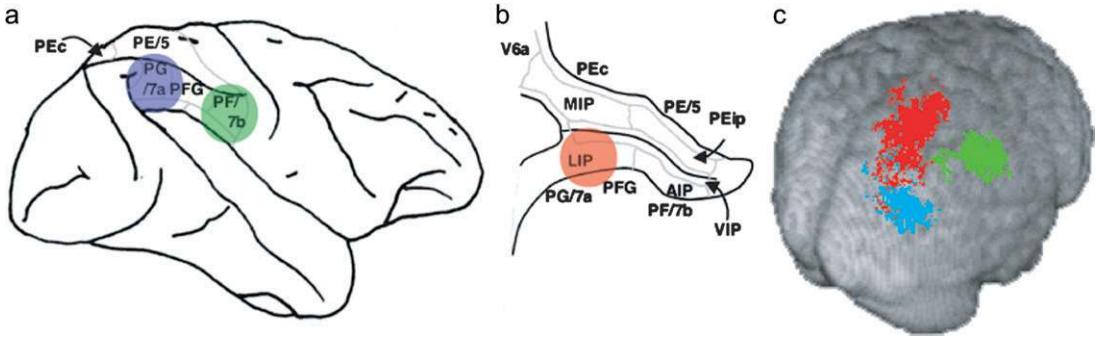

Figure 8. (*a*) The connections of the parahippocampal region (blue), ventral premotor cortex (green), and superior colliculus (red) with the macaque IPL and adjacent lateral bank of the IPS are summarized. (*b*) A similar color scheme is used to summarize the connections of the same 3 regions with the human parietal cortex. Only the points where the connections meet the cortex are shown on the caudal and lateral left hemisphere.

the highest probability of connection was with a region of human IPL, whereas in 1 case, the superior colliculus, the highest probability of connection was with the medial bank of the IPS. The pattern of connectivity highlights both similarities and differences in the organization of parietal cortex in the macaque and human brain. The presence of ventral premotor and parahippocampal projections in the most anterior and posterior IPL regions, respectively, is inconsistent with the view that the entire human IPL is a completely novel structure unrelated to anything found in other primate species. On the other hand, it was noticeable that it was difficult, at least with current DWI tractography techniques, to establish the connection pattern of the middle section of the IPL, and it is this portion of the IPL that is most closely associated with characteristically human behaviors including tool use and calculation (Gruber and others 2001; Johnson-Frey and others 2005). Moreover, it was noticeable that the region with the highest probability of connection with the superior colliculus occupied a relatively medial position. Nevertheless, the superior colliculus–connecting area did not extend throughout the SPL and was mainly confined to the region lateral to the transverse sulcus and the medial bank of the IPS. The area was lateral to the one in which activity is correlated with movement intention and reaching (Rushworth, Paus, and others 2001; Astafiev and others 2003; Connolly and others 2003) and the probabilistic region with the cytoarchitectonic characteristics of area PE (Scheperjans and others 2005) that resembles tissue in the macaque SPL and medial IPS.

In addition to providing new insights into the anatomy of the parietal cortex, the present study suggests that diffusion tractography may complement functional mapping studies in addressing issues of comparative brain anatomy. There are many cortical regions where the relationship between humans and macaques is unclear, but in many cases, the connection patterns of the macaque are well described. The approach employed here could prove generally useful for integrating human brain anatomy with reference to known connection pathways in other species.

Notes

This work was funded by the Medical Research Council and the Royal Society (MFSR) and Biotechnology and Biological Sciences Research Council (HJ-B).

Address correspondence to Matthew Rushworth, Department of Experimental Psychology, South Parks Road, Oxford OX1 3UD, UK. Email: matthew.rushworth@psy.ox.ac.uk.

References

Andersen RA, Asanuma C, Essick G, Siegel RM. 1990. Corticocortical connections of anatomically and physiologically defined subdivisions within the inferior parietal lobule. J Comp Neurol 296:65–113.

Andersen RA, Buneo CA. 2002. Intentional maps in posterior parietal cortex. Annu Rev Neurosci 25:189–220.

Astafiev SV, Shulman GL, Stanley CM, Snyder AZ, Van Essen DC, Corbetta M. 2003. Functional organization of human intraparietal and frontal cortex for attending, looking, and pointing. J Neurosci 23:4689–4699.

Basser PJ, Jones DK. 2002. Diffusion-tensor MRI: theory, experimental design and data analysis—a technical review. NMR Biomed 15:456–467.

Beaulieu C. 2002. The basis of anisotropic water diffusion in the nervous system—a technical review. NMR Biomed 15:435–455.

Behrens TE, Johansen-Berg H, Woolrich MW, Smith SM, Wheeler-Kingshott CA, Boulby PA, Barker GJ, Sillery EL, Sheehan K, Ciccarelli O, Thompson AJ, Brady JM, Matthews PM. 2003. Non-invasive mapping of connections between human thalamus and cortex using diffusion imaging. Nat Neurosci 6:750–757.

Behrens TE, Woolrich MW, Jenkinson M, Johansen-Berg H, Nunes RG, Clare S, Matthews PM, Brady JM, Smith SM. 2003. Characterization and propagation of uncertainty in diffusion-weighted MR imaging. Magn Reson Med 50:1077–1088.

Bender DB, Baizer JS. 1984. Anterograde degeneration in the superior colliculus following kainic acid and radiofrequency lesions of the macaque pulvinar. J Comp Neurol 228:284–298.

Bender DB, Baizer JS. 1990. Saccadic eye movements following kainic acid lesions of the pulvinar in monkeys. Exp Brain Res 79:467–478.

Benevento LA, Fallon JH. 1975. The ascending projections of the superior colliculus in the rhesus monkey (Macaca mulatta). J Comp Neurol 160:339–361.

Binkofski F, Buccino G, Posse S, Seitz RJ, Rizzolatti G, Freund H. 1999. A fronto-parietal circuit for object manipulation in man: evidence from an fMRI-study. Eur J Neurosci 11:3276–3286.

Binkofski F, Buccino G, Stephan KM, Rizzolatti G, Seitz RJ, Freund H-J. 1999. A parieto-premotor network for object manipulation: evidence from neuroimaging. Exp Brain Res 128:210–213.

Binkofski F, Dohle C, Posse S, Stephan KM, Hefter H, Seitz RJ, Freund HJ. 1998. Human anterior intraparietal area subserves prehension: a combined lesion and functional MRI activation study. Neurology 50:1253–1259.

Blatt GJ, Andersen RA, Stoner GR. 1990. Visual receptive field organization and cortico-cortical connections of the lateral intraparietal area (area LIP) in the macaque. J Comp Neurol 299:421–445.

Brodmann K. 1909. Vergleichende Lokalisationslehre der Grosshirnrinde in ihren Prinzipien dargestellt auf Grund des Zellenbaues. Liepzig: J. A. Barth. [Translated by Garey LJ (1994) Localisation in the cerebral cortex. London: Smith-Gordon.]

Cavada C, Goldman-Rakic PS (1989a) Posterior parietal cortex in rhesus monkey: II. Evidence for segregated corticocortical networks linking sensory and limbic areas with the frontal lobe. J Comp Neurol 287:422–445.

Cavada C, Goldman-Rakic PS (1989b) Posterior parietal cortex in rhesus monkey: I. Parcellation of areas based on distinctive limbic and sensory corticocortical connections. J Comp Neurol 287:393–421.

Clemo HR, Stein BE. 1983. Organization of a fourth somatosensory area of cortex in cat. J Neurophysiol 50:910–925.

Clower DM, West RA, Lynch JC, Strick PL. 2001. The inferior parietal lobule is the target of output from the superior colliculus, hippocampus, and the cerebellum. J Neurosci 21:6283–6291.

Colby CL, Duhamel J-R. 1991. Heterogeneity of extrastriate visual areas and multiple parietal areas in the macaque monkey. Neuropsychologia 29:517–537.

Colby CL, Goldberg ME. 1999. Space and attention in parietal cortex. Annu Rev Neurosci 22:319–349.

Collins CE, Lyon DC, Kaas JH. 2005. Distribution across cortical areas of neurons projecting to the superior colliculus in new world monkeys. Anat Rec A Discov Mol Cell Evol Biol 285:619–627.

Collins DL, Neelin P, Peters TM, Evans AC. 1994. Automatic 3D intersubject registration of MR volumetric data in standardized Talairach space. J Comput Assisted Tomogr 18:192–205.

Connolly JD, Andersen RA, Goodale MA. 2003. FMRI evidence for a 'parietal reach region' in the human brain. Exp Brain Res 153:140–145.

Constantinidis C, Steinmetz MA. 2001. Neuronal responses in area 7a to multiple stimulus displays: II. Responses are suppressed at the cued location. Cereb Cortex 11:592–597.

Corbetta M, Akbudak E, Conturo TE, Snyder AZ, Ollinger JM, Drury HA, Linenweber MR, Petersen SE, Raichle ME, Van Essen DC, Shulman GL. 1998. A common network of functional areas for attention and eye movements. Neuron 21:761–773.

Corbetta M, Kincade JM, Ollinger JM, McAvoy MP, Shulman GL. 2000. Voluntary orienting is dissociated from target detection in human posterior parietal cortex. Nat Neurosci 3:292–297.

Corbetta M, Shulman GL. 2002. Control of goal-directed and stimulus-driven attention in the brain. Nat Rev Neurosci 3:201–215.

Croxson PL, Johansen-Berg H, Behrens T, Robson MD, Pinsk MA, Gross C, Richter W, Richter M, Kastner S, Rushworth MFS (2005)

Quantitative investigation of connections of the prefrontal cortex in the human and macaque using probabilistic diffusion tractography. J Neurosci. 25:8854–8866.
de Jong BM, van der Graaf FH, Paans AM. 2001. Brain activation related to the representations of external space and body scheme in visuomotor control. Neuroimage 14:1128–1135.
Devlin JT, Jamison HL, Matthews PM, Gonnerman LM. 2004. Morphology and the internal structure of words. Proc Natl Acad Sci USA 101:14984–14988.
Duvernoy H. 1991. Human brain: surface, three-dimensional sectional anatomy and MRI. New York: Springer Verlag.
Eidelburg D, Galaburda AM. 1984. Inferior parietal lobule: divergent architectonic asymmetries in the human brain. Arch Neurol 41:843–852.
Fink GR, Grefkes C (2005) The functional organization of the intraparietal sulcus in humans and monkeys. J Anat. Forthcoming.
Fries W. 1984. Cortical projections to the superior colliculus in the macaque monkey: a retrograde study using horseradish peroxidase. J Comp Neurol 230:55–76.
Gaymard B, Lynch J, Ploner CJ, Condy C, Rivaud-Pechoux S. 2003. The parieto-collicular pathway: anatomical location and contribution to saccade generation. Eur J Neurosci 17:1518–1526.
Geyer S, Matelli M, Luppino G, Zilles K. 2000. Functional neuroanatomy of the primate isocortical motor system. Anat Embryol 202:443–474.
Gitelman DR, Nobre AC, Parrish TB, LaBar KS, Kim YH, Meyer JR, Mesulam M. 1999. A large scale distributed network for covert spatial attention: further anatomical delineation based on stringent behavioural and cognitive controls. Brain 122:1093–1106.
Glickstein M. 2003. Subcortical projections of the parietal lobes. Adv Neurol 93:43–55.
Glover S. 2004. Separate visual representations in the planning and control of action. Behav Brain Sci 27:3–24; discussion 24–78.
Grefkes C, Weiss PH, Zilles K, Fink GR. 2002. Crossmodal processing of object features in human anterior intraparietal cortex: an fMRI study implies equivalencies between humans and monkeys. Neuron 35:173–184.
Grefkes C, Fink GR. 2005. The functional organization of the intraparietal sulcus in humans and monkeys. J. Anat. 207:3–17.
Grosbras MH, Laird AR, Paus T. 2005. Cortical regions involved in eye movements, shifts of attention, and gaze perception. Hum Brain Mapp 25:140–154.
Gruber O, Indefrey P, Steinmetz H, Kleinschmidt A. 2001. Dissociating neural correlates of cognitive components in mental calculation. Cereb Cortex 11:350–359.
Hagmann P, Thiran JP, Jonasson L, Vandergheynst P, Clarke S, Maeder P, Meuli R. 2003. DTI mapping of human brain connectivity: statistical fibre tracking and virtual dissection. Neuroimage 19:545–554.
Hardy SGP, Lynch JC. 1992. The spatial distribution of pulvinar neurons that project to two subregions of the inferior parietal lobule in the macaque. Cereb Cortex 2:217–230.
Jenkinson M, Smith S. 2001. A global optimisation method for robust affine registration of brain images. Med Image Anal 5:143–156.
Johansen-Berg H, Behrens TE, Robson MD, Drobnjak I, Rushworth MFS, Brady JM, Smith SM, Higham DJ, Matthews PM. 2004. Changes in connectivity profiles define functionally distinct regions in human medial frontal cortex. Proc Natl Acad Sci USA 101:13335–13340.
Johansen-Berg H, Behrens TE, Sillery E, Ciccarelli O, Thompson AJ, Smith SM, Matthews PM. 2005. Functional-anatomical validation and individual variation of diffusion tractography-based segmentation of the human thalamus. Cereb Cortex 2005 15:31–39.
Johnson-Frey SH, Newman-Norlund R, Grafton ST. 2005. A distributed left hemisphere network active during planning of everyday tool use skills. Cereb Cortex 15:681–695.
Jones DK, Simmons A, Williams SC, Horsfield MA. 1999. Non-invasive assessment of axonal fiber connectivity in the human brain via diffusion tensor MRI. Magn Reson Med 42:37–41.
Kincade JM, Abrams RA, Astafiev SV, Shulman GL, Corbetta M. 2005. An event-related functional magnetic resonance imaging study of voluntary and stimulus-driven orienting of attention. J Neurosci 25:4593–4604.
Koyama M, Hasegawa I, Osada T, Adachi Y, Nakahara K, Miyashita Y. 2004. Functional magnetic resonance imaging of macaque monkeys performing visually guided saccade tasks: comparison of cortical eye fields with humans. Neuron 41:795–807.
Lavenex P, Suzuki WA, Amaral DG. 2002. Perirhinal and parahippocampal cortices of the macaque monkey: projections to the neocortex. J Comp Neurol 447:394–420.
Lawler KA, Cowey A. 1987. On the role of posterior parietal and prefrontal cortex in visuo-spatial perception and attention. Exp Brain Res 65:695–698.
Lehericy S, Ducros M, Krainik A, Francois C, Van de Moortele PF, Ugurbil K, Kim DS. 2004. 3-D diffusion tensor axonal tracking shows distinct SMA and pre-SMA projections to the human striatum. Cereb Cortex 14:1302–1309.
Lock TM, Baizer JS, Bender DB. 2003. Distribution of corticotectal cells in macaque. Exp Brain Res 151:455–470.
Lynch JC, Graybiel AM, Lobeck LJ. 1985. The differential projection of two cytoarchitectonic subregions of the inferior parietal lobule of macaque upon the deep layers of the superior colliculus. J Comp Neurol 235:241–254.
Lynch JC, McLaren J. 1989. Deficits of visual attention and saccadic eye movements after lesions of parietoccipital cortex in monkeys. J Neurophysiol 61:74–90.
Makris N, Kennedy DN, McInerney S, Sorensen AG, Wang R, Caviness VS Jr, Pandya DN. 2005. Segmentation of subcomponents within the superior longitudinal fascicle in humans: a quantitative, in vivo, DT-MRI study. Cereb Cortex 15:854–869.
Matelli M, Camarda R, Glickstein M, Rizzolatti G. 1986. Afferent and efferent projections of the inferior area 6 in the macaque monkey. J Comp Neurol 251:281–298.
Mori S, Kaufmann WE, Davatzikos C, Stieltjes B, Amodei L, Fredericksen K, Pearlson GD, Melhem ER, Solaiyappan M, Raymond GV, Moser HW, van Zijl PC. 2002. Imaging cortical association tracts in the human brain using diffusion-tensor-based axonal tracking. Magn Reson Med 47:215–223.
Mort DJ, Malhotra P, Mannan SK, Rorden C, Pambakian A, Kennard C, Husain M (2003) The anatomy of visual neglect. Brain 126: 1986–1997.
Mort DJ, Perry RJ, Mannan SK, Hodgson TL, Anderson E, Quest R, McRobbie D, McBride A, Husain M, Kennard C (2003) Differential cortical activation during voluntary and reflexive saccades in man. Neuroimage 18:231–246.
Mufson EJ, Pandya DN. 1984. Some observations on the course and composition of the cingulum bundle in the rhesus monkey. J Comp Neurol 225:31–43.
Nobre AC, Sebestyen GN, Gitelman DR, Mesulam MM, Frackowiak RSJ, Frith CD. 1997. Functional localization of the system for visuospatial attention using positron emission tomography. Brain 120:515–533.
Pandya DP, Seltzer B. 1982. Intrinsic connections and architectonics of posterior parietal cortex in the rhesus monkey. J Comp Neurol 204:196–210.
Parker GJ, Alexander DC. 2003. Probabilistic Monte Carlo based mapping of cerebral connections utilising whole-brain crossing fibre information. Inf Process Med Imaging 18:684–695.
Petrides M, Pandya D. 2002. Association pathways of the prefrontal cortex and functional observations. In: Stuss DT, Knight RT, editors. Principles of frontal lobe function. New York: Oxford University Press. p 31–50.
Pruessner JC, Kohler S, Crane J, Pruessner M, Lord C, Byrne A, Kabani N, Collins DL, Evans AC. 2002. Volumetry of temporopolar, perirhinal, entorhinal and parahippocampal cortex from high-resolution MR images: considering the variability of the collateral sulcus. Cereb Cortex 12:1342–1353.
Rushworth MFS, Ellison A, Walsh V. 2001. Complementary localization and lateralization of orienting and motor attention. Nat Neurosci 4:656–661.
Rushworth MFS, Johansen-Berg H, Young SA. 1998. Parietal cortex and spatial-postural transformation during arm movements. J Neurophysiol 79:478–482.
Rushworth MFS, Krams M, Passingham RE. 2001. The attentional role of the left parietal cortex: the distinct lateralization and localization of motor attention in the human brain. J Cogn Neurosci 13:698–710.

Rushworth MFS, Nixon PD, Passingham RE (1997a) The parietal cortex and movement. I. Movement selection and reaching. Exp Brain Res 117:292–310.
Rushworth MFS, Nixon PD, Passingham RE (1997b) Parietal cortex and movement. II. Spatial representations. Exp Brain Res 117: 311–323.
Rushworth MFS, Paus T, Sipila PK. 2001. Attention systems and the organization of the human parietal cortex. J Neurosci 21:5262–5271.
Sakata H, Taira M, Kusunoki M, Murata A, Tanaka Y. 1997. The TINS lecture. The parietal association cortex in depth perception and visual control of hand action. Trends Neurosci 20:350–357.
Sakata H, Taira M, Kusunoki M, Murata A, Tsutsui K, Tanaka Y, Shein WN, Miyashita Y. 1999. Neural representation of three dimensional features of manipulation objects with stereopsis. Exp Brain Res 128:160–169.
Scheperjans F, Grefkes C, Palomero-Gallagher N, Schleicher A, Zilles K. 2005. Subdivisions of human parietal area 5 revealed by quantitative receptor autoradiography: a parietal region between motor, somatosensory, and cingulate cortical areas. Neuroimage 25:975–992.
Seltzer B, Pandya DN. 1984. Further observations on parieto-temporal connections in the rhesus monkey. Exp Brain Res 55:301–312.
Seltzer B, Pandya DN. 1986. Posterior parietal projections to the intraparietal sulcus of the rhesus monkey. Exp Brain Res 62:459–469.
Sereno MI, Pitzalis S, Martinez A. 2001. Mapping of contralateral space in retinotopic coordinates by a parietal cortical area in humans. Science 294:1350–1354.
Sereno MI, Tootell RB. 2005. From monkeys to humans: what do we now know about brain homologies? Curr Opin Neurobiol 15:135–144.
Shikata E, Hamzei F, Glauche V, Koch M, Weiller C, Binkofski F, Buchel C. 2003. Functional properties and interaction of the anterior and posterior intraparietal areas in humans. Eur J Neurosci 17:1105–1110.
Silver MA, Ress D, Heeger DJ. 2005. Topographic maps of visual spatial attention in human parietal cortex. J Neurophysiol. 94:1358–1371.
Smith SM. 2002. Fast robust automated brain extraction. Hum Brain Mapp 17:143–155.
Steinmetz MA, Constantinidis C. 1995. Neurophysiological evidence for a role of posterior parietal cortex in redirecting visual attention. Cereb Cortex 5:448–456.
Stieltjes B, Kaufmann WE, van Zijl PC, Fredericksen K, Pearlson GD, Solaiyappan M, Mori S. 2001. Diffusion tensor imaging and axonal tracking in the human brainstem. Neuroimage 14:723–735.
Suzuki WA, Amaral DG. 1994. Perirhinal and parahippocampal cortices of the macaque monkey: cortical afferents. J Comp Neurol 350:497–533.
Thiel CM, Zilles K, Fink GR. 2004. Cerebral correlates of alerting, orienting and reorienting of visuospatial attention: an event-related fMRI study. Neuroimage 21:318–328.
Thiel CM, Zilles K, Fink GR. 2005. Nicotine modulates reorienting of visuospatial attention and neural activity in human parietal cortex. Neuropsychopharmacology 30:810–820.
Tournier JD, Calamante F, Gadian DG, Connelly A. 2003. Diffusion-weighted magnetic resonance imaging fibre tracking using a front evolution algorithm. Neuroimage 20:276–288.
Tuch DS, Reese TG, Wiegell MR, Wedeen VJ. 2003. Diffusion MRI of complex neural architecture. Neuron 40:885–895.
Von Bonin G, Bailey P. 1947. The neocortex of Macaca mulatta. Urbana, IL: University of Illinois Press.
Wallace MT, Meredith MA, Stein BE. 1993. Converging influences from visual, auditory, and somatosensory cortices onto output neurons of the superior colliculus. J Neurophysiol 69:1797–1809.
Zhang Y, Brady M, Smith S. 2001. Segmentation of brain MR images through a hidden Markov random field model and the expectation-maximization algorithm. IEEE Trans Med Imaging 20:45–57.